

Patterns due to an interplay between viscous and precipitation-driven fingering

F. Haudin and A. De Wit

Citation: *Physics of Fluids* **27**, 113101 (2015); doi: 10.1063/1.4934669

View online: <http://dx.doi.org/10.1063/1.4934669>

View Table of Contents: <http://scitation.aip.org/content/aip/journal/pof2/27/11?ver=pdfcov>

Published by the [AIP Publishing](#)

Articles you may be interested in

[Chemical precipitation structures formed by drops impacting on a deep pool](#)

J. Chem. Phys. **137**, 184701 (2012); 10.1063/1.4762828

[Colloidal electroconvection in a thin horizontal cell. III. Interfacial and transient patterns on electrodes](#)

J. Chem. Phys. **137**, 014504 (2012); 10.1063/1.4730752

[Atomization patterns produced by the oblique collision of two Newtonian liquid jets](#)

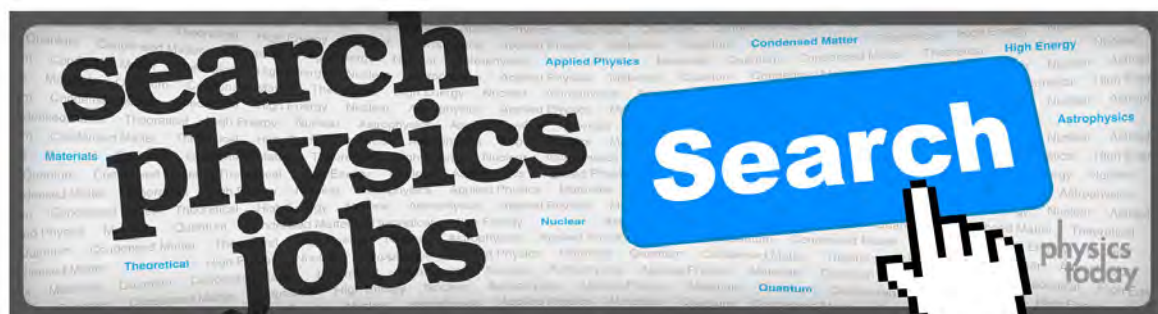
Phys. Fluids **22**, 042101 (2010); 10.1063/1.3373513

[Miscible viscous fingering involving viscosity changes of the displacing fluid by chemical reactions](#)

Phys. Fluids **22**, 024101 (2010); 10.1063/1.3301244

[Mixing in a drop moving through a serpentine channel: A computational study](#)

Phys. Fluids **17**, 073305 (2005); 10.1063/1.1992514



Patterns due to an interplay between viscous and precipitation-driven fingering

F. Haudin and A. De Wit

*Université libre de Bruxelles (ULB), Nonlinear Physical Chemistry Unit,
Faculté des Sciences, CP231, 1050 Brussels, Belgium*

(Received 4 January 2015; accepted 14 October 2015; published online 2 November 2015)

Dynamics related to the interplay of viscous fingering with precipitation-driven patterns are studied experimentally in a horizontal Hele-Shaw cell with radial injection. The precipitation reaction, known to produce chemical gardens, involves a cobalt chloride metallic salt solution and a more viscous sodium silicate one. The properties of the fingering precipitation patterns are studied as a function of the flow rate of injection, of the viscosity ratio between the two solutions and of the concentration of the reactants. We show that, for the viscous silicate solution used here, viscous fingering shapes flower-like patterns at low metallic salt concentrations but is not the driving mechanism in the development of spirals and filaments at larger cobalt chloride concentrations. In some cases, enhanced convective motions induced by viscous fingering also increase the amount of precipitate by increasing the mixing between the two reactants. © 2015 AIP Publishing LLC. [<http://dx.doi.org/10.1063/1.4934669>]

I. INTRODUCTION

Fingering of an interface upon displacement of one fluid by another one typically arises when mobility decreases along the direction of the flow. This is the case when a less viscous, more mobile fluid displaces another more viscous and hence less mobile one in porous media. The interface between the two fluids deforms then into fingers because of a viscous fingering instability, which has been thoroughly studied both experimentally and theoretically.¹ Fingering can also occur because of a change in mobility induced by a dissolution of a porous matrix² or because of a precipitation between two reactive solutions leading locally to a decrease in permeability.^{3–6} In some cases, like typically in mineralization processes during CO₂ injection in soils for sequestration purposes, both precipitation reactions⁷ as well as viscous fingering⁸ phenomena may occur simultaneously. We investigate here the fingering patterns arising when such precipitation processes interplay with the viscous fingering (VF) instability in miscible displacements.

The coupling between non precipitation reactions and miscible VF has already been the focus of several works. Bistable autocatalytic reactions have, for instance, been shown numerically to allow for rupture of fingers into isolated droplets.^{9–11} Nagatsu and collaborators have next performed extended experimental analysis of VF characteristics in the presence of $A + B \rightarrow C$ type of reactions modifying *in situ* the viscosity of the solutions. They have shown that the properties of the viscous fingers depend on whether the reaction increases or decreases the viscosity and whether the reaction is instantaneous or proceeds with a finite characteristic time.^{12–15} Reactions impacting viscosity have also been shown experimentally to trigger fingering patterns between reactant solutions of same viscosity¹⁶ and even in the initially stable case of a more viscous polymer solution displacing a reactive less viscous aqueous solution.¹⁷ From the theoretical point of view, a classification of the various viscous fingering instability scenarii in the case of isothermal $A + B \rightarrow C$ or exothermic autocatalytic traveling waves¹⁹ has been performed by linear stability analysis. Numerical simulations have analyzed the nonlinear dynamics of related reactive viscous fingering.^{19–23}

Recently, Nagatsu *et al.*²⁴ have started studying experimentally viscous fingering dynamics in presence of a precipitation type of reaction. To do so, they analyze the patterns observed when a

solid precipitate C is formed by a precipitation reaction $A + B \rightarrow C_{(s)}$ in the miscible contact zone between an aqueous solution of reactant A displacing more viscous glycerin containing the reactant B.²⁴ They showed that, for a moderate precipitation concentration, finger splitting decreases to favour the formation of straight-shaped fingers. For high precipitation concentrations, bending of fingers in an almost perpendicular direction was observed.

For reactive solutions of same viscosities, it has recently been shown both experimentally and theoretically that a local decrease of permeability in a local precipitation zone can trigger fingering.³ For another precipitation reaction in confined geometries, i.e., a chemical garden involving aqueous solutions of cobalt chloride CoCl_2 and sodium silicate, a large variety of patterns including flowers, filaments, and worms was further evidenced.⁴⁻⁶ In these systems, viscous effects can operate as well for high concentrations of silicate.

In this context, we investigate here experimentally the fingering patterns that can arise when precipitation processes interplay with the VF instability in miscible displacements. To do so, we analyze the relative contribution of viscous effects and of the precipitation reaction in the patterns formed upon radial injection of aqueous solutions of cobalt chloride into silicate in variable concentrations in a horizontal confined geometry. We show that viscous effects are important in shaping the form of flower-like structures while they are not the driving mechanism in the case of spirals and filaments. We also provide quantitative tools to characterize the growth of these various patterns.

The article is organized as follows: we first describe in Section II the setup of the experiments and give information on the chemicals used. We next analyze the relative interplay of viscous and precipitation effects in the properties of flower-like patterns in Section III while those of spirals and filaments are discussed in Section IV. Quantitative information on the growth properties of these various structures is given in Section V before conclusions are drawn.

II. EXPERIMENTAL SETUP

The precipitation reaction considered here belongs to the family of reactions producing chemical gardens in 3D beakers, i.e., tubular structures obtained when a metallic salt is poured as a solid crystal seed into a waterglass solution,²⁵⁻²⁹ this name being commonly used to refer to a sodium silicate solution. The chemical garden dynamics, known from the 17th century, involve a cooperative action of buoyancy, reaction-diffusion processes, and osmosis. When a seed of a metallic salt is poured in a beaker containing an alkaline solution like sodium silicate, carbonate or potassium phosphate to name a few, a semi-permeable membrane forms around the seed. The water of the outside solution is pumped in by osmosis, ensuring then a further dissolution of the salt till the rupture of the membrane, followed by the ejection of a buoyant jet of generally less dense acidic metallic salt solution inside the alkaline reservoir. Along this jet, further precipitation occurs, producing tubular structures with generally complex shapes. If instead of a seed or a pellet, an aqueous solution of such metallic salts is injected in a container filled with the silicate solution, other complex 3D growth dynamics are obtained.^{30,31} Here, we analyze the dynamics during injection in the quasi 2D geometry of a horizontal Hele-Shaw cell, which allows for reduction of osmotic and buoyancy effects.^{4,32} The cell is made of two Plexiglass plates (215 mm \times 215 mm \times 8 mm) separated by a small gap (0.5 mm) thanks to a plastic sheet. Two syringe pumps have been used: either a Razel or a KD Scientific 200. The range of flow rates accessible with the KD scientific pump mainly used is limited to 83 ml/min in the conditions of the experiments. The injected reactant is cobalt chloride in concentration C_1 produced by dissolution in water of $\text{CoCl}_2 \cdot 6\text{H}_2\text{O}$ (Sigma Aldrich). The displaced reactant is a sodium silicate solution of concentration C_2 prepared by dilution of a commercial solution (Sigma Aldrich) at 6.25M with respect to silica concentration. The radial injection is performed from the center of the cell at a given constant flow rate q . Table I reports the viscosities μ_1 and μ_2 of the injected metallic salt and displaced silicate solutions, respectively, along with the related log-mobility ratios $R = \ln(\mu_2/\mu_1)$ for different concentrations.

When the cobalt chloride is injected into the silicate one, precipitation occurs in the mixing zone. Let us analyze the various patterns obtained as well as the relative importance of viscous and precipitation effects in their properties for various concentrations.

TABLE I. Concentration C_1 and related viscosity μ_1 of the injected cobalt chloride solutions along with the related log-mobility ratios $R = \ln(\mu_2/\mu_1)$ and viscosity μ_2 in the case of a displaced silicate solution in concentration $C_2 = 3.13\text{M}$ (third line) and $C_2 = 6.25\text{M}$ (fourth line). All measurements are performed at room temperature.

C_1 (M)	0	0.10	0.25	0.63	1.00	1.38
μ_1 (mPa s)	1	1.1	1.2	1.4	1.6	1.7
R ($\mu_2 = 3.6$ mPa s)	1.3	1.2	1.1	0.9	0.8	0.8
R ($\mu_2 \approx 40$ mPa s)	3.7	3.6	3.5	3.4	3.2	3.2

III. INFLUENCE OF VISCOUS FINGERING ON FLOWER-TYPE PRECIPITATES

For small concentrations of the injected metallic salt solution and a viscous suspension of concentrated silicate ($R = 3.6$), a flower-like pattern influenced by underlying viscous fingering is observed (Fig. 1(a)). In this reference experiment, we see that, initially, the precipitate develops inside the viscous fingers (Fig. 1(a1)). After about 9 s, the precipitate does no longer follow the growth of the fingers but stays behind them (Fig. 1(a2)). The discrepancy between the viscous fingers and the precipitate location is increasing with time as visible in Fig. 1(a3). In most experiments presented here, the injected solutions also contain a blue food dye (Vahiné), supposed passive and not changing the fingering dynamics. It enables to visualize the region of the injected fluid in non reactive cases or when the cobalt chloride is very diluted and almost transparent. As an example, Figs. 1(a) and 1(b) show the same experiment with non-dyed and dyed solutions of cobalt chloride, respectively.

To show the influence of viscous fingering on the shape of the precipitate pattern, the effect of decreasing by half the flow rate for the non-dyed cobalt chloride solution is displayed in Fig. 1(c). Unsurprisingly, decreasing the flow rate leads to a larger wavelength of the underlying viscous fingers, that also develop more slowly, in agreement with the fact that a displacement is less unstable with regard to VF when the injection speed is decreased.^{33,34} Viscous effects decrease as well when the concentration, and hence viscosity, of the silicate solution is decreased (Fig. 1(d), $R = 1.2$). We thus see that growing chemical gardens by injecting CoCl_2 into a viscous concentrated silicate solution in a Hele-Shaw cell can lead to quite complex patterns that result from the occurrence of both viscous fingering and precipitation-driven phenomena. The interplay between these two sources of instabilities is intricate and varies with the amount of precipitate formed (depending on the relative concentrations of reactants), the flow rate q , and the viscosity ratio (equivalently the silicate concentration) between the two reactant solutions. Let us now study successively the effect of changes of these various parameters on the flower pattern to disentangle the relative contribution of viscous and precipitation effects on the dynamics.

First, to understand the effect of viscous fingering on the dynamics, we analyze the patterns in absence of the precipitation reaction by injecting dyed water or glycerol inside the silicate solutions of different concentrations (Figs. 2(a) and 2(b)). If the silicate is concentrated such that $R = 3.7$, a classical viscous fingering instability is observed (Fig. 2(a)) when water is injected in it. Both mixing zones in Figs. 1(a) and 2(a) are deformed into fingers, signature of a large enough viscosity contrast between the injected and displaced fluids, even if their specific features are different. If the silicate concentration is decreased such that the viscosity ratio is much lower, no viscous fingering is observed (Fig. 2(b)). The log-mobility ratio $R = 1.2$ is not sufficient at that speed of injection to deform the mixing zone into fingers before reaching the edges of the cell. Alternatively, the viscosity ratio can also be reduced by adding glycerol to the injected solution. The equi-viscosity case of both solutions at 40 mPa s ($R \sim 0$) is shown in Fig. 2(c) for dyed diluted glycerol injected into concentrated silicate. The contact zone between the two fluids remains circular and only very thin little buoyancy-driven stripes³⁵ develop at the rim visible when zooming on the cell⁶ (indistinguishable in the field of view here). The displacement has reached a smaller distance at the same time than in the stable water/silicate injection of Fig. 2(b) due to the larger viscosity of the injected glycerol. Indeed, within the gap of the cell, the shape of the injected fluid tongue depends on the

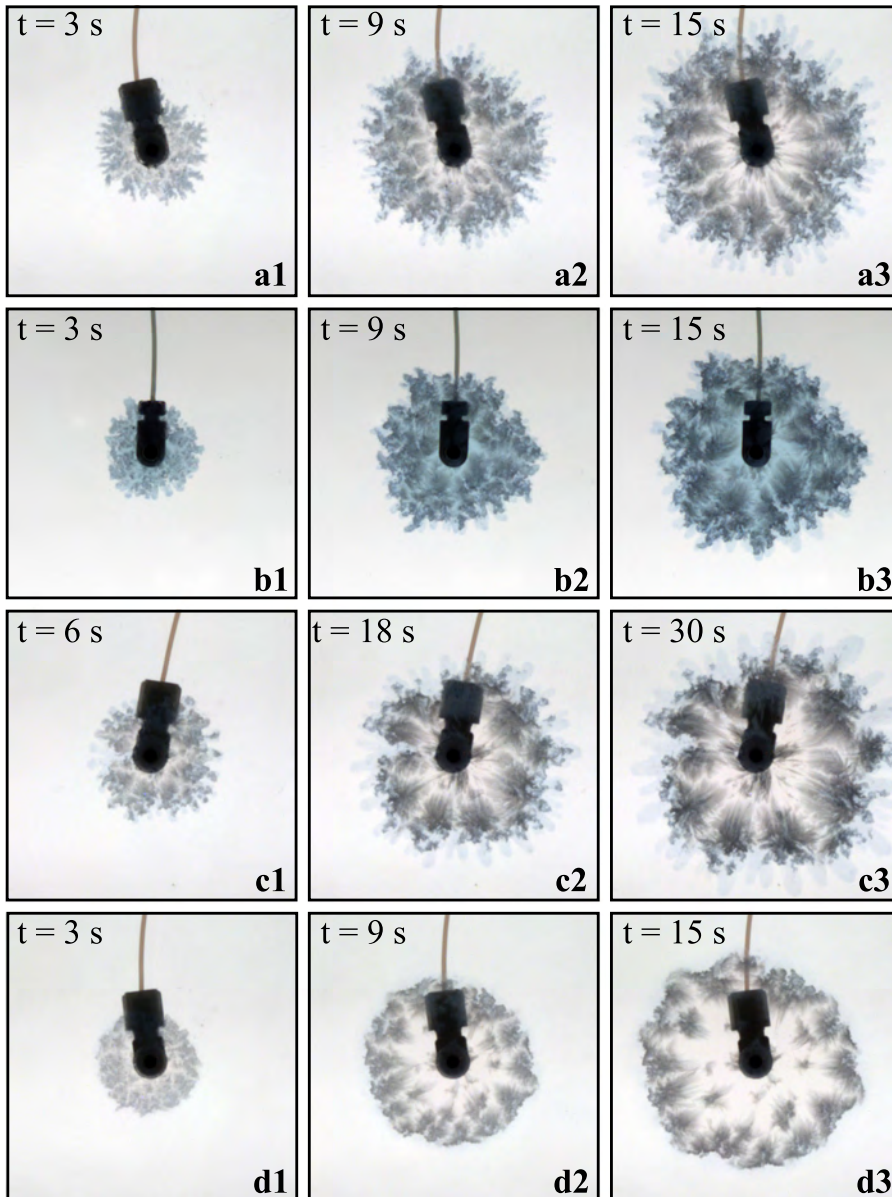


FIG. 1. Experimental patterns for miscible displacements of sodium silicate ($C_2 = 6.25\text{M}$) by (a) an aqueous solution of cobalt chloride ($C_1 = 0.1\text{M}$, $R = 3.6$, $q = 6.5$ ml/min), (b) same as (a) but with a blue dye added in the injected cobalt chloride, (c) effect of decreasing the flow rate: same as (a) but $q = 3.4$ ml/min, (d) effect of decreasing the sodium silicate concentration to $C_2 = 3.13\text{M}$, $R = 1.2$, with $q = 6.5$ ml/min. The field of view is $10\text{ cm} \times 10\text{ cm}$.

relative density and viscosity of the two fluids.^{35,36} A reactive case at equal viscosity is shown in Fig. 2(d) when a glycerol solution of cobalt chloride 0.1M is injected into concentrated silicate. In that case, the contact zone between the two solutions remains viscously stable and a homogeneous precipitation occurs inside the circle. A comparison of Figs. 1(b) and 2(d) shows that, at equal reactant concentrations of CoCl_2 and silicate and same flow rate, the amount of precipitate is much larger in the case affected by VF (Fig. 1(b)) than in the case of the viscously stable displacement in presence of glycerol (Fig. 2(d)). This suggests that the enhanced convective motions triggered by VF³⁷ increase the reaction yield by increasing the mixing between the two reactants while only a homogeneous low concentration precipitate is formed in the case of the stable displacement.

To further elucidate the effect of VF on the precipitation pattern, we can also keep the viscosity ratio constant ($R = 3.6$) using aqueous solutions of CoCl_2 injected into viscous concentrated silicate

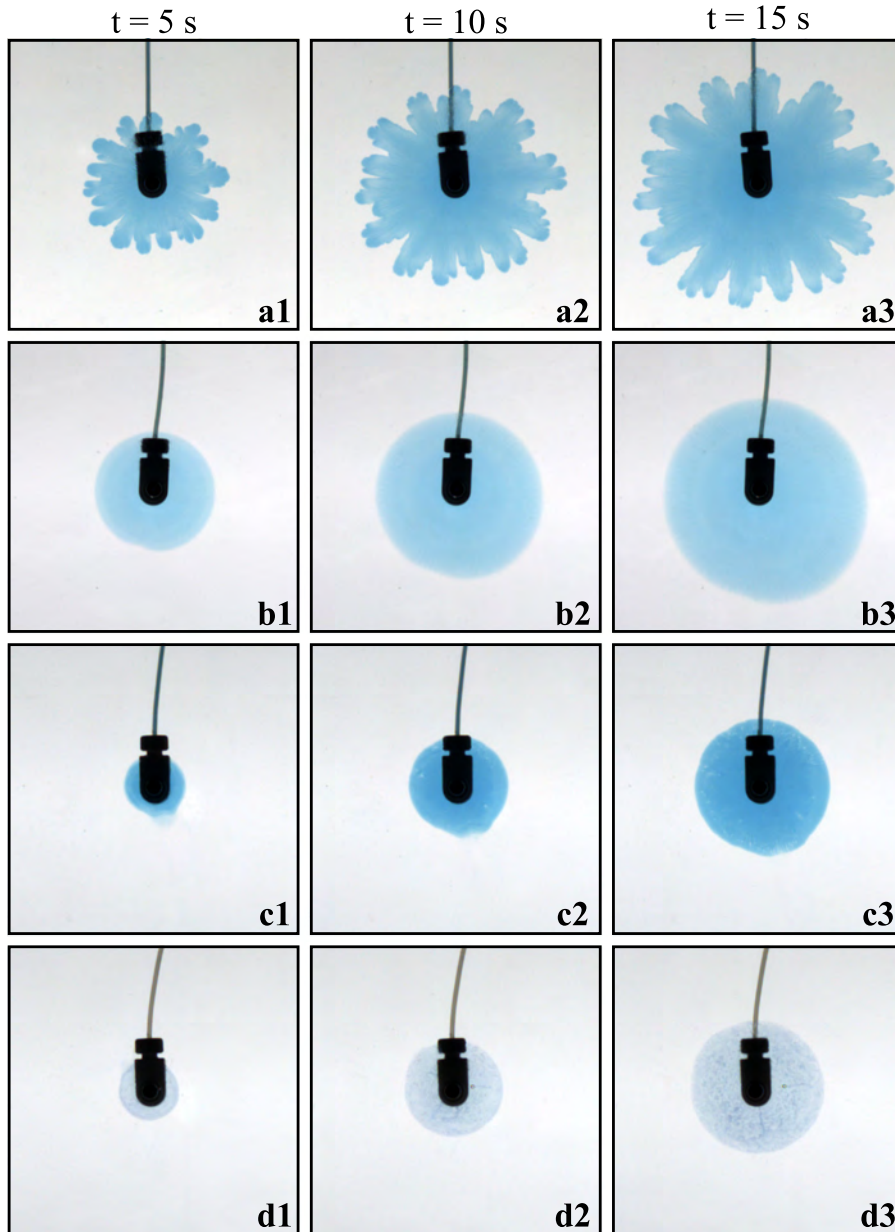


FIG. 2. Miscible displacements of (a) dyed water inside concentrated sodium silicate at $R=3.7$ ($C_2=6.25\text{M}$), (b) dyed water inside more diluted sodium silicate for $R=1.2$ ($C_2=3.13\text{M}$), (c) dyed glycerol ($\approx 76\%$ in weight to reach a viscosity close to 40 mPa s) inside concentrated sodium silicate ($C_2=6.25\text{M}$, i.e., $R\sim 0$), and (d) same as in (c) with cobalt chloride ($C_1=0.1\text{M}$) dissolved in the glycerol. The flow rate is 6.5 ml/min and the field of view is $10\text{ cm} \times 10\text{ cm}$.

6.25M , and tune the injection rate as done in Fig. 3. Here, the flow rate is varied on more than two orders of magnitude (between 0.1 and 65 ml/min) for comparable injected volumes. In the following Table II, the range of Reynolds and Péclet numbers explored when changing the flow rates is estimated. The definitions chosen for Re and Pe numbers are the following:¹²

$$Re = \rho_2 U b / \mu_2 = \rho_2 q / (2\pi R \mu_2), \quad (1)$$

$$Pe = U b / D = q / (2\pi R D), \quad (2)$$

with q the flow rate, $U = q / (2\pi R b)$ the speed of injection, b the thickness of the cell, R the radial distance from the injection point taken as 2 cm , $\rho_2 = 1.42\text{ g cm}^{-3}$, and $\mu_2 \approx 40\text{ mPa s}$, respectively, the density and the viscosity of the displaced reactant solution, and $D = 10^{-9}\text{ m}^2/\text{s}$ an estimate of the

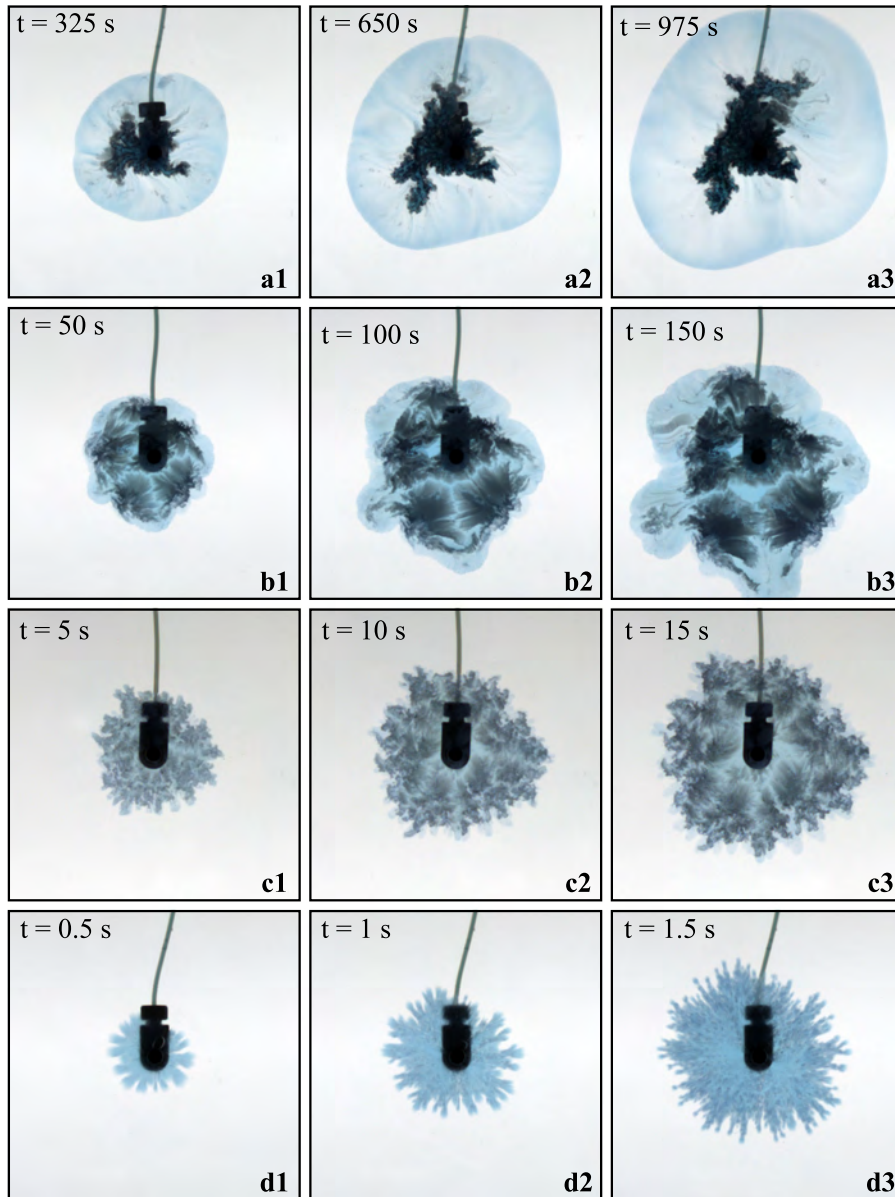


FIG. 3. Fingering patterns for miscible displacements at $R=3.6$ of viscous sodium silicate ($C_2=6.25\text{M}$) by an aqueous solution of dyed cobalt chloride solution ($C_1=0.1\text{M}$) for 4 different flow rates: (a) $q=0.1$ ml/min, (b) $q=0.65$ ml/min, (c) $q=6.5$ ml/min, and (d) $q=65$ ml/min. For each column, the volume of injected reactant is the same. The field of view is $10\text{ cm} \times 10\text{ cm}$.

molecular diffusion coefficient. We can see that the Reynolds numbers range from 10^{-4} to close to 10^{-2} , indicating that the flow remains in Stokes flow conditions. The Pe numbers vary from small to large values such that diffusive effects are expected to be important at the lowest flow rate while advective transport is dominant at the largest flow rate.

Analyzing the experimental results, quite logically, a smaller time is needed to inject the same volume when the flow rate is decreased (along a column of Fig. 3). For $q=0.1$ ml/min (Fig. 3(a)), there is no viscous fingering developing since the speed of injection is too small. The dynamics is so slow that the system behaves like in a diffusive regime with a liquid zone growing ahead almost circularly and a branching green precipitate developing behind it, close to the injection point. For $q=0.65$ ml/min (Fig. 3(b)), the pattern looks similar to the flower of the reference case at $q=6.5$ ml/min (added for comparison in Fig. 3(c)) but the characteristic wavelength of

TABLE II. Estimates of the Reynolds number Re and of the Péclet number Pe for flow rates in Fig. 3.

	Re	Pe
$q = 0.1$ ml/min	4.6×10^{-4}	13.3
$q = 6.5$ ml/min	3.0×10^{-2}	864.5

the finger is much larger as the system is viscously less unstable. The precipitation occurs inside the liquid by agglomeration at given locations forming bunches of dark solid. For the larger flow rate $q = 65$ ml/min (Fig. 3(d)), the wavelength of the underlying viscous finger is much smaller and the injection is so quick that there is less precipitation inside the fingers than for flow rates 10 or 100 times smaller. This suggests that there exists a critical speed above which VF is observed in our Hele-Shaw cell and that there is an optimum intermediate speed at which the amount of precipitate is maximum. At large injection speed, VF dominates the dynamics, the advective flow takes over diffusion which hinders a good mixing of fresh reactants and a formation of much more precipitate. In intermediate regimes, the solid produced catches up the progression of the liquid advancing rim and the pattern results from a combination of VF and precipitation. This suggests that an important parameter of the problem to be considered in future modelling is the Damköhler number, i.e., the ratio between the characteristic hydrodynamic time t_{hydro} based on the injection speed and of the reactive time t_{reac} . This number is difficult to estimate here as the details of the reactions and kinetic constants are not known. Nevertheless, as the reaction can be considered as instantaneous ($t_{reac} \ll t_{hydro}$), the Damköhler number should be quite large, except perhaps for the larger flow rates, for which the two times start to be in the same range.

To study the effect of precipitation on a given VF reference case, we can also tune the concentration C_1 of the injected cobalt chloride solution for a fixed large concentration C_2 of the viscous silicate solution. We see in Fig. 4(a) that, when $C_1 = 0.01$ M, there is not much difference between the non reactive case (Fig. 2(a)) and this one, suggesting that the amount of precipitate formed is negligible. For $C_1 = 0.05$ M (Fig. 4(b)), the amount of precipitate is increased. In that case, the viscous fingers and the related solid petals of flowers are less developed than in the $C_1 = 0.1$ M case (Fig. 1(b)). Obviously, the viscous and precipitation-driven instabilities have an influence one onto the other, which is a function of the reactant concentration ratio $\phi = C_2/C_1$.

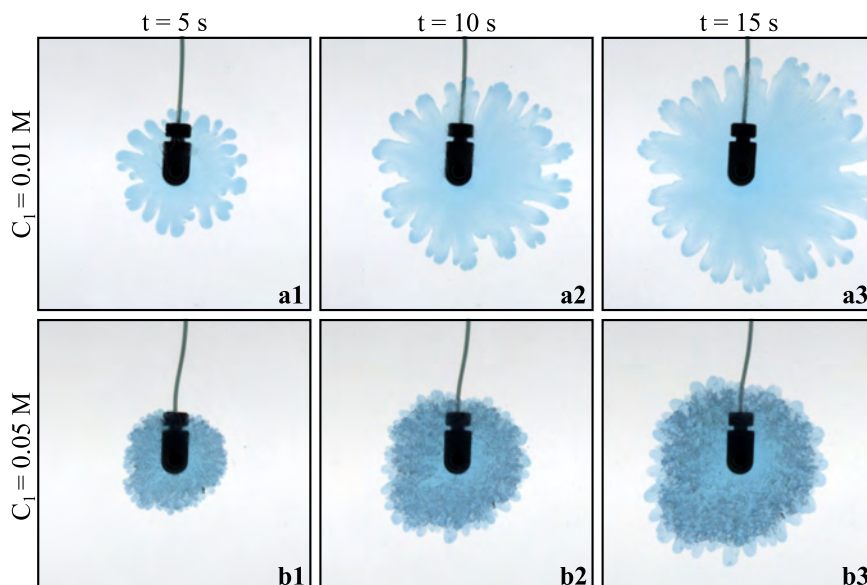


FIG. 4. Change of pattern for $R \sim 3.7$ as a function of the concentration of cobalt chloride: (a) $C_1 = 0.01$ M and (b) $C_1 = 0.05$ M. The flow rate is 6.5 ml/min, $C_2 = 6.25$ M, and the field of view is 10 cm \times 10 cm.

To conclude the analysis of the effect of varying the concentration of the metallic salt solution, we find that, at low CoCl_2 concentration, the solid particles are not produced in sufficient amount to influence the hydrodynamics. As a result, the VF pattern looks similar with or without precipitation. It is only above a given amount of solid produced that the reactive and non reactive patterns start to differ, once the precipitation affects the flow. It is difficult to quantify for which value of concentration sufficient difference between reactive and non reactive cases occurs and whether the transition is monotonic or not. Further investigations are needed to answer such questions.

IV. SPIRALS AND FILAMENTS

It has been shown previously that, for aqueous solutions of CoCl_2 and silicate at $C_2 = 6.25\text{M}$ for which the log-mobility ratio is large (see Table I), spirals are observed at $C_1 = 0.25\text{M}$ while tiny twisted filaments are obtained for $C_1 \geq 0.63\text{M}$.⁴ The fact that spirals are obtained for the same viscosity ratio ($R = 3.6$) as flowers and, more generally, in a large zone of the concentration parameter space⁴ with smaller values of R , points to the fact that viscous effects are not crucial to their formation. The spiraling precipitates can actually be understood in terms of a minimal geometrical model based on the displacement of a solid initially circular wall upon breaking at a given point because of injection.⁴

Let us here explore intermediate concentrations of CoCl_2 for viscous silicate 6.25M to see if the transition between flowers, spirals, and filaments is smooth or not (Fig. 5). For $C_1 = 0.15\text{M}$, a flower-like pattern made of structures reminiscent of spirals is observed (Fig. 5(a)). In the quantitative analysis of Section V, we will see that they can be classified in the spiral category considering certain criteria. A zoom-in on a similar pattern taken a few minutes after the end of the injection is shown in Fig. 6(a) which reveals a majority of dark blue precipitate containing some notes of green-turquoise in some places. For $C_1 = 0.20$ and 0.25M , the patterns are composed of spirals (Figs. 5(b) and 5(c)). For $C_1 = 0.35\text{M}$, the global pattern is in between spirals and filaments with channels made of smaller spirals (Fig. 5(d)). When C_1 is further increased, the injected fluid produces two types of structures: either small filamentous structures of type F1 (shown in Fig. 5(e) for $C_1 = 0.45\text{M}$ and on a zoom in on these structures few minutes after the end of injection on Fig. 6(b)), or filaments with larger structures looking like balloons blowing locally (Fig. 5(f), $C_1 = 0.55\text{M}$) that we call filaments of type F2. Finally, for $C_1 = 0.63\text{M}$, F1 filaments with transitions to larger F2 structures are observed (Fig. 5(g)). It is interesting to note that for $C_1 = 0.63\text{M}$, there can be either F2 structures that are close to worm patterns reported in Ref. 4 but with thicker walls (Fig. 5(g)), a mixing of F1 and F2 filaments (Fig. 5(h)), or only the F1 type (Fig. 5(i)) depending on the experiments. This shows that, for the same set of experimental conditions, a bistability between the two F1 and F2 types can be obtained. For larger C_1 concentrations, a third type F3 of filaments can also be observed, with locally straight contours paving the available space.⁶

Patterns looking similar to the worms and filaments (and also to some secondary structures of the hair patterns observed in the confined chemical garden experiments in Ref. 4) have been previously reported: some patterns referred to as tentacles have for instance been observed for a reaction producing a gel in the contact zone between two reactants of same viscosity.¹⁶ They grow in a similar way as directional fingers investigated by Nagatsu *et al.* in experiments involving both viscous fingering and precipitation²⁴ or gel formation.³⁸

To check to what extent the filament structures depend on the viscosity ratio between the two solutions, we further compare the patterns obtained when CoCl_2 is injected in more concentrated silicate solutions (Figs. 5(g)-5(i)) with the structures observed for a more viscous solution CoCl_2 with sucrose displacing the same silicate solution ($C_2 = 5\text{M}$) (Fig. 7(b)). Experimentally, the cobalt chloride solution is prepared at the suitable concentration and then by progressive addition of sucrose and successive viscosity measurements, the viscosity is increased above the one of the outer silicate solution. The control is thus not made on the concentration of sucrose but on the viscosity of the solution. In both viscously stable and unstable cases, filaments are obtained (Fig. 7). Even if their width is variable, the fact that they can be obtained in these various cases points to the fact that the viscosity of the injected or displaced solutions does not seem to be a key factor in the development of filaments.

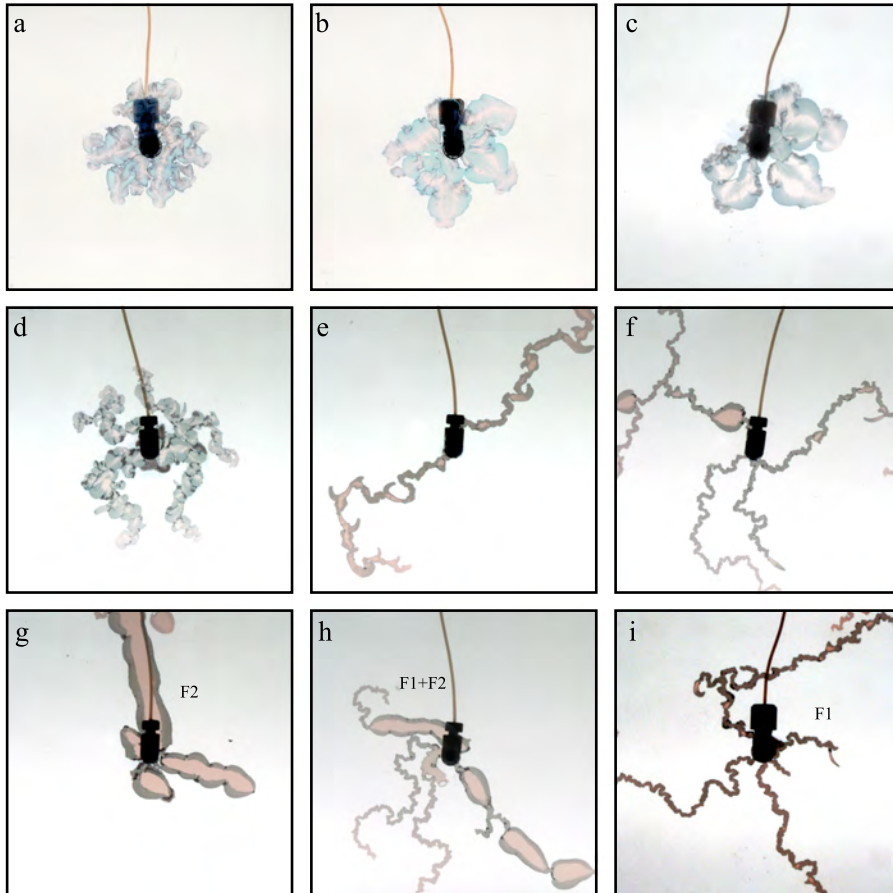


FIG. 5. Transition between different patterns for $C_2=6.25M$ and different concentrations C_1 : (a) 0.15M, (b) 0.20M, (c) 0.25M, (d) 0.35M, (e) 0.45M, (f) 0.55M, (g)-(i) 0.63M ($R \sim 3.4-3.5$). The pictures are taken 15 s after the beginning of the injection, the flow rate is 6.5 ml/min and the field of view is $15 \text{ cm} \times 15 \text{ cm}$.

V. QUANTITATIVE CHARACTERIZATION OF PATTERNS

Quantitative information on the dynamics of the structures can be extracted to get insight in the way the precipitates are growing and distributed in space. To do so, the pictures resulting from one channel of the RGB experimental snapshots (usually the blue one, which is the most contrasted one for the pink CoCl_2) are binarized according to a threshold chosen to suitably capture

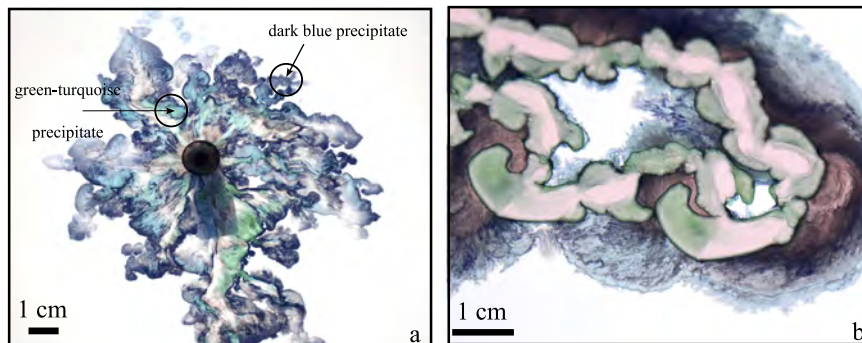


FIG. 6. Zoom in on the structures, (a) intermediate between the flowers and the spirals ($C_1=0.15M$), (b) with boomerang shapes existing for concentrations between those of spirals and filaments ($C_1=0.45M$). The photograph are taken few minutes after the end of the injection.

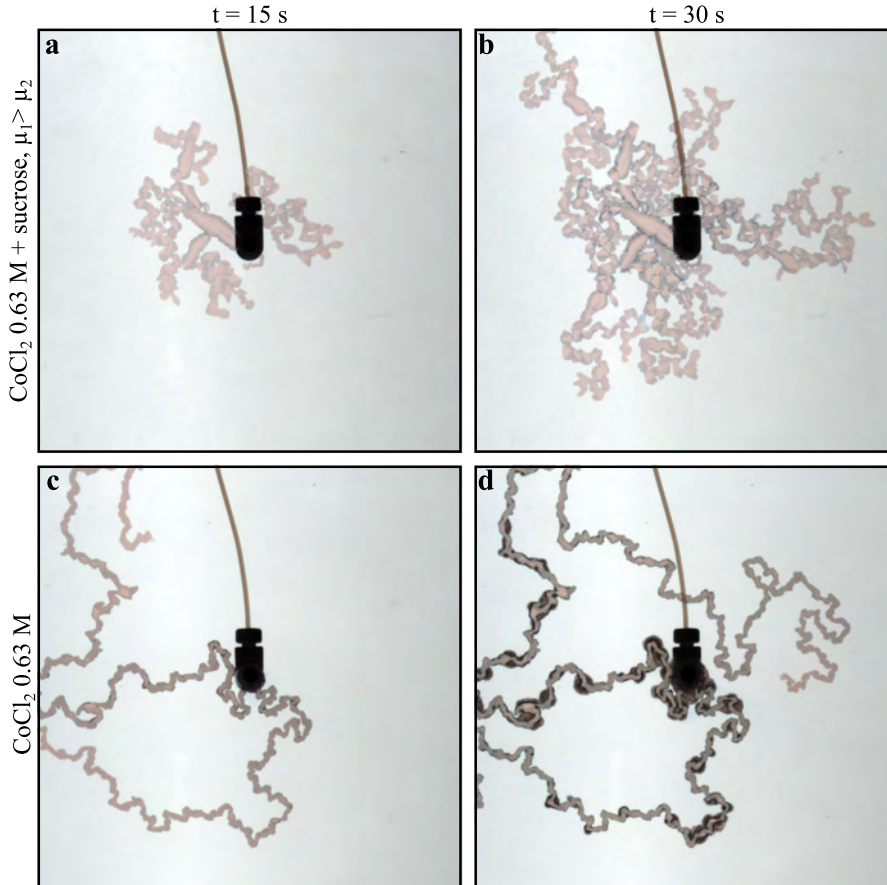


FIG. 7. Influence of the viscosity ratio on the filaments. (a) and (b) viscously stable injection of a viscous aqueous solution of sucrose and cobalt chloride 0.63M inside less viscous sodium silicate 5M ($\mu_1 \approx 23$ mPa s, $\mu_2 \approx 13$ mPa s, $R = -0.6$); (c) and (d) injection of cobalt chloride 0.63M inside sodium silicate 5M ($\mu_1 \approx 1.4$ mPa s, $\mu_2 \approx 13$ mPa s, $R = 2.2$). Filaments are observed in both cases suggesting that the viscosity difference is not a key factor in their formation. The flow rate is 6.5 ml/min and the field of view is 15 cm \times 15 cm.

the area \mathcal{A} of the injected reactant and of the precipitate part. If the precipitate forms within the cell with vertical walls enclosing the injected reactant, then the evolution of the area should scale as $\mathcal{A}(t) = \mathcal{V}(t)/b = q \cdot t/b$ with \mathcal{V} the injected volume. Fig. 8(a) shows the temporal evolution of \mathcal{A} for various concentrations of both reactants. The plots for the 24 reported experiments are distributed around the line $q \cdot t/b$. Some dispersion exists due to errors on the thickness of the cell and on the flow rate and also on data processing due to the presence of the injector on the image and of the subjective choice of the binarizing threshold. Note that, for the concentrations $C_1 = 0$ or 0.1M, the threshold is applied to the red channel of the pictures since the peripheric viscous fingers are rather blue. The smaller areas correspond to patterns intermediate between spirals and filaments for which different layers not necessarily spanning the whole gap are observed. Also, for the filaments, \mathcal{A} are underestimated as soon as they start growing outside the analysis window (smaller than the total cell extent). Nevertheless, we see that the areas grow linearly in time in good approximation for most structures showing that most of the patterns studied here span approximately the gap width of the cell during their growth.

The temporal evolution of the radial extent of the structures is computed in Fig. 8(b) showing the radius R_{max} of the circle passing by the furthest point of the precipitate pattern from the injection hole. The evolution of R_{max} gives an information about how fast the structures grow.¹² Three main trends emerge: flowers and spirals are slow growing patterns, the structures made of a mixture of spirals and filaments have an intermediate growth velocity while the filaments are the patterns that

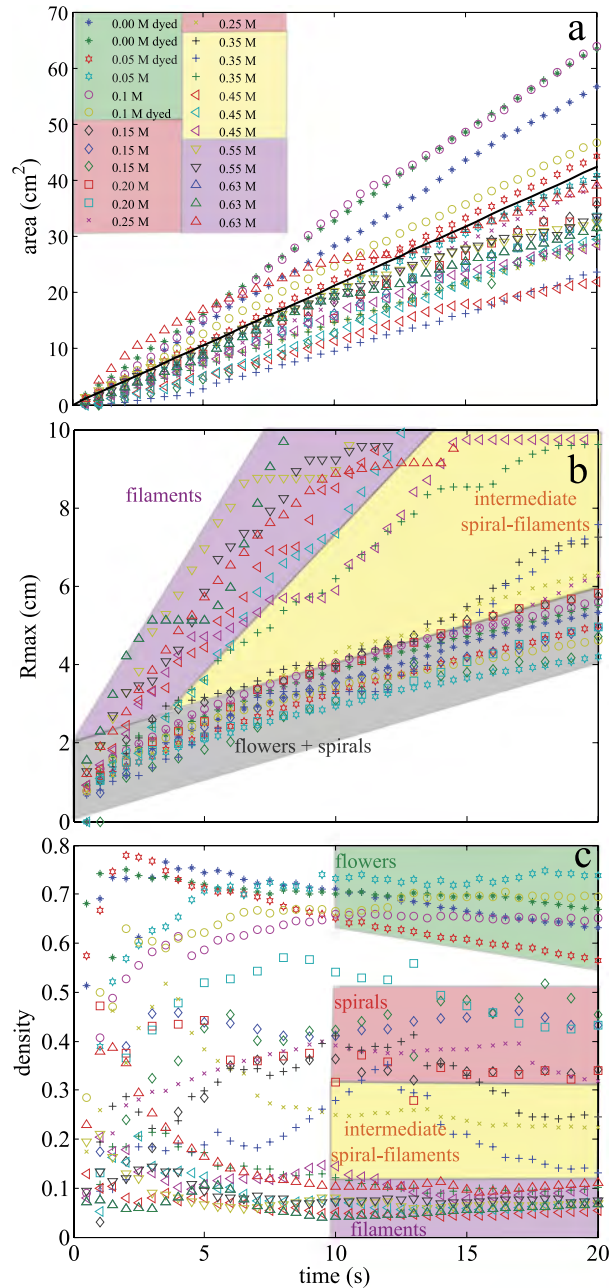


FIG. 8. Time evolution of (a) the area \mathcal{A} of the injected fluid and precipitate, (b) R_{\max} , and (c) the pattern density d for concentrations C_1 ranging from 0 to 0.63M for the cobalt chloride solution ($C_2 = 6.25\text{M}$ for the sodium silicate). In (a), the solid line represents the fit qt/b . The flow rate is 6.5 ml/min for all experiments. The different colors in the inserts correspond to the different categories of patterns : filaments (violet), intermediates between filaments and spirals (yellow), spirals (red) and flowers (green).

most quickly reach the boundaries of the cell. For filaments, R_{\max} saturate to a maximum value when they get out of the analysis window.

We can also compute a pattern density $d = \mathcal{A}/\pi R_{\max}^2$ (Fig. 8(c)) which gives the percentage of the area of the circle of radius R_{\max} covered by the area \mathcal{A} of both the injected reactant and the precipitate.¹² This pattern density gives information on how compact the pattern is, with a perfectly radial growth without any destabilization giving the largest density equal to 1. We see that d converges in time towards three distinct average values depending whether the structures are the most

compact flowers or purely viscous fingers (d between 0.55 and 0.8), spirals (d between 0.3 and 0.5), or filaments (smallest value of the density around 0.1) for which R_{max} is evolving fast (Fig. 8(b)). Increasing the concentration of the metallic salt at a fixed large concentration of silicate thus leads to a less and less compact pattern. Such curves can be a good tool for classifying the different patterns.

VI. CONCLUSIONS

In conclusion, we have investigated the displacement of a viscous silicate solution by a cobalt chloride one in a horizontal Hele-Shaw cell to analyze the relative contribution of viscous and precipitation-driven fingering in the pattern selection. We have analyzed the effect of the injection flow rate, of the viscosity ratio between both solutions and of the concentrations of the reactants on the selected structures. We find that, for large silicate but lower CoCl_2 concentrations, the displacement is viscously unstable providing flowers in which the precipitate pattern is influenced by the viscous fingers. When the cobalt chloride concentration is progressively increased the pattern is switching to spirals and then progressively to filaments, the properties of which appear to be independent of the viscosity ratio. We have quantitatively characterized the geometrical growth of the structures showing that they approximately span the gap of the cell and that filaments grow much more rapidly with a smaller pattern density than the spirals and flowers, respectively. These results pave the way to understand how the coupling between flow instabilities and precipitation reactions can be used to select given specific precipitate structures.

ACKNOWLEDGMENTS

We thank F. Brau, J. Cartwright, O. Steinbock, and V. Brasiliense for fruitful discussions and PRODEX for financial support. A.D. also acknowledges support from the FORECAST FRS-FNRS research project.

- ¹ G. M. Homsy, "Viscous fingering in porous media," *Annu. Rev. Fluid Mech.* **19**, 271 (1987).
- ² C. Wei and P. Ortoleva, "Reaction front fingering in carbonate-cemented sandstones," *Earth-Sci. Rev.* **29**, 183 (1990).
- ³ Y. Nagatsu, Y. Ishii, Y. Tada, and A. De Wit, "Hydrodynamic fingering instability induced by a precipitation reaction," *Phys. Rev. Lett.* **113**, 024502 (2014).
- ⁴ F. Haudin, J. H. E. Cartwright, F. Brau, and A. De Wit, "Spiral precipitation patterns in confined chemical gardens," *Proc. Nat. Acad. Sci. U. S. A.* **111**, 17363 (2014).
- ⁵ F. Haudin, J. H. E. Cartwright, and A. De Wit, "Direct and reverse chemical garden patterns grown upon injection in confined geometries," *J. Phys. Chem. C* **119**, 15067 (2015).
- ⁶ F. Haudin, V. Brasiliense, J. H. E. Cartwright, F. Brau, and A. De Wit, "Genericity of confined chemical garden patterns with regard to changes in the reactants," *Phys. Chem. Chem. Phys.* **17**, 12804 (2015).
- ⁷ C. Zhang, K. Dehoff, N. Hess, M. Oostrom, T. W. Wietsma, A. J. Valocchi, B. W. Fouke, and C. J. Werth, "Pore-scale study of transverse mixing induced by CaCO_3 precipitation and permeability reduction in a model subsurface sedimentary system," *Environ. Sci. Technol.* **44**, 7833 (2010).
- ⁸ S. Berg and H. Ott, "Stability of CO_2 brine immiscible displacement," *Int. J. Greenhouse Gas Control* **11**, 188 (2012).
- ⁹ A. De Wit and G. M. Homsy, "Viscous fingering in reaction-diffusion systems," *J. Chem. Phys.* **110**, 8663 (1999).
- ¹⁰ A. De Wit and G. M. Homsy, "Nonlinear interactions of chemical reactions and viscous fingering in porous media," *Phys. Fluids* **11**, 949 (1999).
- ¹¹ K. Ghesmat and J. Azaiez, "Miscible displacements of reactive and anisotropic dispersive flows in porous media," *Transp. Porous Media* **77**, 489 (2009).
- ¹² Y. Nagatsu, K. Matsuda, Y. Kato, and Y. Tada, "Experimental study on miscible viscous fingering involving viscosity changes induced by variations in chemical species concentrations due to chemical reactions," *J. Fluid Mech.* **571**, 475 (2007).
- ¹³ Y. Nagatsu, Y. Kondo, Y. Kato, and Y. Tada, "Effects of moderate Damköhler number on miscible viscous fingering involving viscosity decrease due to a chemical reaction," *J. Fluid Mech.* **625**, 97 (2009).
- ¹⁴ Y. Nagatsu, C. Iguchi, K. Matsuda, Y. Kato, and Y. Tada, "Miscible viscous fingering involving viscosity changes of the displacing fluid by chemical reactions," *Phys. Fluids* **22**, 024101 (2010).
- ¹⁵ Y. Nagatsu, Y. Kondo, Y. Kato, and Y. Tada, "Miscible viscous fingering involving viscosity increase by a chemical reaction with moderate Damköhler number," *Phys. Fluids* **23**, 014109 (2011).
- ¹⁶ T. Podgorski, M. C. Sostarecz, S. Zorman, and A. Belmonte, "Fingering instabilities of a reactive micellar interface," *Phys. Rev. E* **76**, 016202 (2007).
- ¹⁷ L. A. Riolfo, Y. Nagatsu, S. Iwata, R. Maes, P. M. J. Trevelyan, and A. De Wit, "Experimental evidence of reaction-driven miscible viscous fingering," *Phys. Rev. E* **85**, 015304(R) (2012).
- ¹⁸ S. H. Hejazi, P. M. J. Trevelyan, J. Azaiez, and A. De Wit, "Viscous fingering of a miscible reactive $A + B \rightarrow C$ interface: A linear stability analysis," *J. Fluid Mech.* **652**, 501 (2010).

- ¹⁹ S. Swernath and S. Pushpavanam, "Viscous fingering in a horizontal flow through a porous medium induced by chemical reactions under isothermal and adiabatic conditions," *J. Chem. Phys.* **127**, 204701 (2007).
- ²⁰ T. Gérard and A. De Wit, "Miscible viscous fingering induced by a simple $A + B \rightarrow C$ chemical reaction," *Phys. Rev. E* **79**, 016308 (2009).
- ²¹ S. H. Hejazi and J. Azaiez, "Non-linear interactions of dynamic reactive interfaces in porous media," *Chem. Eng. Sci.* **65**, 938 (2010).
- ²² S. H. Hejazi and J. Azaiez, "Hydrodynamic instability in the transport of miscible reactive slices through porous media," *Phys. Rev. E* **81**, 056321 (2010).
- ²³ Y. Nagatsu and A. De Wit, "Viscous fingering of a miscible reactive $A + B \rightarrow C$ interface for an infinitely fast chemical reaction: Nonlinear simulations," *Phys. Fluids* **23**, 043103 (2011).
- ²⁴ Y. Nagatsu, S.-K. Bae, Y. Kato, and Y. Tada, "Miscible viscous fingering with a chemical reaction involving precipitation," *Phys. Rev. E* **77**, 0067302 (2008).
- ²⁵ R. D. Coatman, N. L. Thomas, and D. D. Double, "Studies of the growth of 'silicate gardens' and related phenomena," *J. Mater. Sci.* **15**, 2017 (1980).
- ²⁶ L. M. Barge, S. S. S. Cardoso, J. H. E. Cartwright, G. J. T. Cooper, L. Cronin, A. De Wit, I. J. Doloboff, B. Escribano, R. E. Goldstein, F. Haudin, D. E. H. Jones, A. L. Mackay, J. Maselko, J. J. Pagano, J. Pantaleone, M. J. Russell, C. Ignacio Sainz-Díaz, O. Steinbock, D. A. Stone, Y. Tanimoto, and N. L. Thomas, "From chemical gardens to chemiobryonics," *Chem. Rev.* **115**, 8652-8703 (2015).
- ²⁷ J. H. E. Cartwright, J. M. Garcia-Ruiz, M. L. Novella, and F. Otalora, "Formation of chemical gardens," *J. Colloid Interface Sci.* **256**, 351 (2002).
- ²⁸ J. H. E. Cartwright, B. Escribano, and C. I. Sainz-Díaz, "Chemical-garden formation, morphology, and composition. I. Effect of the nature of the cations," *Langmuir* **27**, 3286 (2011).
- ²⁹ A. Tóth, D. Horváth, R. Smith, J. R. McMahan, and J. Maselko, "Phase diagram of precipitation morphologies in the Cu^{2+} - PO_4^{3-} system," *J. Phys. Chem. C* **111**, 14762 (2007).
- ³⁰ S. Thouvenel-Romans and O. Steinbock, "Oscillatory growth of silica tubes in chemical gardens," *J. Am. Chem. Soc.* **125**, 4338 (2003).
- ³¹ J. J. Pagano, S. Thouvenel-Romans, and O. Steinbock, "Compositional analysis of copper-silica precipitation tubes," *Phys. Chem. Chem. Phys.* **9**, 110 (2007).
- ³² O. Steinbock, "Complexity from precipitation reactions," *Proc. Natl. Acad. Sci. U. S. A.* **111**, 17346 (2014).
- ³³ C. T. Tan and G. M. Homsy, "Stability of miscible displacements in porous media: Rectilinear flow," *Phys. Fluids* **29**, 3549 (1986).
- ³⁴ C. T. Tan and G. M. Homsy, "Simulation of nonlinear viscous fingering in miscible displacement," *Phys. Fluids* **31**, 1330 (1988).
- ³⁵ F. Haudin, L. A. Riolfo, B. Knaepen, G. M. Homsy, and A. De Wit, "Experimental study of a buoyancy-driven instability of a miscible horizontal displacement in a Hele-Shaw cell," *Phys. Fluids* **26**, 044102 (2014).
- ³⁶ N. Rakotomalala, D. Salin, and P. Watzky, "Miscible displacement between two parallel plates: BGK lattice gas simulations," *J. Fluid Mech.* **338**, 277 (1997).
- ³⁷ B. Jha, L. Cueto-Felgueroso, and R. Juanes, "Fluid mixing from viscous fingering," *Phys. Rev. Lett.* **106**, 194502 (2011).
- ³⁸ Y. Nagatsu, A. Hayashi, M. Ban, Y. Kato, and Y. Tada, "Spiral pattern in a radial displacement involving a reaction-producing gel," *Phys. Rev. E* **78**, 026307 (2008).